



0008-8846(95)00048-8

## GENERAL HYDRATION MODEL FOR PORTLAND CEMENT AND BLAST FURNACE SLAG CEMENT

G. DE SCHUTTER

Research Assistant of the Belgian National Fund for Scientific Research (N.F.W.O.)  
Magnet Laboratory for Concrete Research, Ghent, Belgium

L. TAERWE

Professor, Magnet Laboratory for Concrete Research, Ghent, Belgium

(Refereed)

(Received May 1; in final form October 5, 1994)

**ABSTRACT :** This paper focusses on the evolution of the heat of hydration of hardening concrete or cement based materials. Based on isothermal and adiabatic hydration tests a new general hydration model is developed, valid both for portland cement and blast furnace slag cement. This hydration model enables the calculation of the heat production rate as a function of the actual temperature and the degree of hydration.

### 1. INTRODUCTION

The hydration of cement is an exothermic process. Due to the heat of hydration thermal gradients occur inside massive concrete elements, causing thermal stresses which may reach considerable values. Early age thermal crack formation might yield a loss of function (e.g. water tightness of tunnel walls) or a reduction of service life (e.g. concrete armour units) (1).

At the University of Ghent a finite element program for the prediction of thermal stresses due to the heat of hydration in hardening concrete elements is being developed (1,2). The main purpose of the whole project is the prediction of residual stresses and crack formation in massive concrete structures, and the influence on durability.

This contribution focusses on the evolution of the heat of hydration. Up to now hydration models have only been proposed for Portland cement. As for massive concrete elements blast furnace slag cement is used frequently, a new hydration model also valid for this type of cement is needed.

### 2. EXPERIMENTAL DETERMINATION OF THE HEAT OF HYDRATION

#### 2.1. Isothermal hydration tests on cement : conduction calorimetry

Conduction calorimetry appears to be a useful technique for examining the hydration

behaviour of different types of cement (3). A description of the conduction method can be found in several national codes, e.g. the Belgian Standard NBN B12-213.

The test is performed on a cement paste with water/cement ratio equal to 0.5. Measurement of the heat production rate  $q$  (in J/gh) takes place continuously starting immediately after water addition. This enables the registration of the first peak of the heat production, i.e. the peak occurring in the first minutes after the water addition (Figure 1). However, in the interpretation of the test results (see further) this first peak is not considered because of measuring problems caused by very small temperature differences between the cement paste and the water bath at the beginning of the test. Furthermore, the integrated contribution of the first peak (total heat  $Q$  in J/g) only amounts to a few percent of  $Q_{\max}$ , being the total heat liberated at complete cement hydration. Finally, as in practice concrete isn't cast immediately after water addition, the heat corresponding with the first peak is never produced inside the concrete element. The first peak "remains in the concrete mixer" and only contributes to a slightly higher initial temperature. The effect of the first peak could be compared to the added mechanical energy due to mixing, and is considered implicitly in the casting temperature of the concrete. For portland cement the total heat  $Q_{\max}$  can be calculated from the Bogue composition. For slag cement (and for portland cement) an approximate value can always be obtained experimentally by means of isothermal hydration tests.

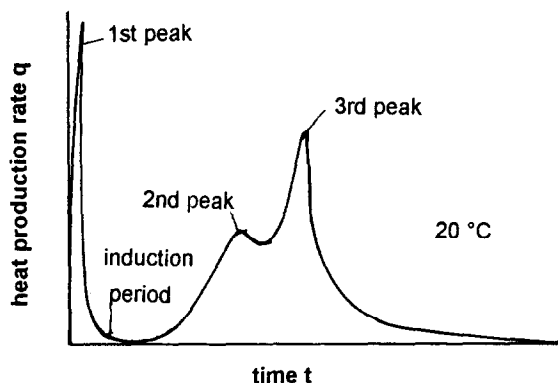


FIG. 1  
Heat of hydration

At the Belgian Research Centre of the Cement Industry isothermal hydration tests were performed on three different kinds of cements (portland cement CEM I 52.5, blast furnace slag cements CEM III/B 32.5 and CEM III/C 32.5) at three different temperatures (5, 20, 35°C). The chemical composition and the fineness of the cements is given in table 1.

## 2.2. Adiabatic hydration tests on concrete

With adiabatic hydration tests the heat production rate  $q$  can be calculated by measuring the temperature rise of the perfectly insulated concrete, as a function of the time. An easy implementation would be the measurement of the core temperature of insulated, very massive concrete cubes. However, a small calculation shows that, with an expanded polystyrene insulation of 100 mm, and a test period of 5 to 7 days, a concrete cube with side length 2 m is needed to get a maximum heat loss of a few percent. This is confirmed by test results given in (4). In order to avoid concrete volumes of this kind, an alternative, though much more complicated test method was developed, as indicated in Figure 2. Around a cylindrical concrete specimen (diameter 280 mm, height 400 mm) a water ring is created. By means of

TABLE 1  
Chemical Composition (in %) and Fineness

	CEM I 52.5	CEM III/B 32.5	CEM III/C 32.5
$\text{SiO}_2$	19.92	26.76	27.12
$\text{Al}_2\text{O}_3$	5.02	7.33	9.40
$\text{Fe}_2\text{O}_3$	3.39	2.52	1.63
CaO	63.75	50.54	42.95
MgO	0.96	5.61	7.23
Blaine ( $\text{cm}^2/\text{g}$ )	5054	4380	4500

a differential thermostat, connected with a heating element, the water ring is kept at the same temperature as the concrete. In this way the concrete is maintained in adiabatic conditions. Although theoretically there is no need to place an insulation between concrete and water, preliminary experiments pointed out that for practical reasons it is a necessity. An air-ring seemed to be the ideal solution, because of its high insulating value and its small specific heat.

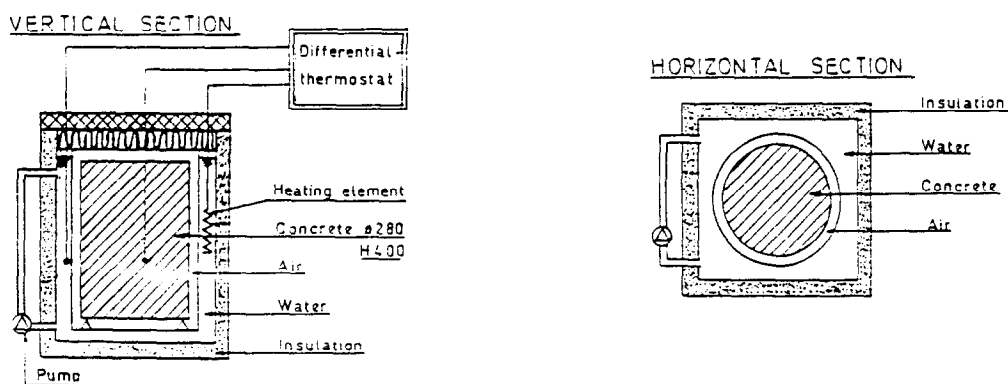


FIG. 2  
Adiabatic hydration test

At the Magnel Laboratory for Concrete Research adiabatic hydration tests were performed on concrete consisting per  $\text{m}^3$  of 300 kg cement, 150 kg water, 670 kg sand and 1280 kg gravel. The tests were carried out with the same cement types as mentioned earlier. Some characteristics of the fresh and hardened concrete are mentioned in table 2.

### 3. RESULTS OF ISOTHERMAL HYDRATION TESTS

#### 3.1. Portland cement CEM I 52.5

As mentioned earlier, the hydration tests were performed at three different temperatures : 5, 20 and 35°C. Figure 3 gives the heat production rate  $q$  (without first peak) for portland cement CEM I 52.5 as a function of time  $t$ . A more fundamental parameter is the degree of

TABLE 2  
Concrete Properties

Cement	Fresh Concrete			Hardened Concrete (cubes 158 mm)	
	Slump (mm)	Flow (-)	Density (kg/m <sup>3</sup> )	Density (kg/m <sup>3</sup> )	Mean cube strength 28 days (N/mm <sup>2</sup> )
CEM I 52.5	14	1.27	2420	2410	64.8
CEM III/B 32.5	38	1.43	2420	2380	39.7
CEM III/C 32.5	35	1.47	2400	2360	20.4

hydration  $\alpha$ , defined as the cement fraction that has reacted. Due to difficulties in experimentally determining the degree of hydration  $\alpha$ , it is often approximated by the degree of reaction  $r$ , defined as the fraction of the heat of hydration that has been released.

$$r(t) = \frac{Q(t)}{Q_{\max}} = \frac{1}{Q_{\max}} \int_0^t q(t) dt \quad (1)$$

Transforming the time axis  $t$  of Figure 4 into a degree of reaction axis  $r$ , Figure 4 is obtained. The curves, corresponding to the different temperatures, are quite similar in shape. This is even more remarkable when the values of each curve are divided by its maximum value  $q_{\max}$ , as indicated in Figure 5. The standardized curves  $q/q_{\max}$  seem to be independent of the temperature  $\theta$ . This was already indicated by Reinhardt et al. (5). The obtained curves can be described mathematically as follows :

$$\frac{q}{q_{\max}} = f(r) = c \cdot [\sin(r\pi)]^a \cdot \exp(-br) \quad (2)$$

For the tested portland cement, the constants in the expression are found to be

$$a = 0.667 \quad , \quad b = 3.0 \quad ; \quad c = 2.5968$$

The temperature effect can be described separately by a temperature function  $g(\theta)$

$$q_{\max} = q_{\max,20} \cdot g(\theta) \quad (3)$$

with  $q_{\max,20} = q_{\max}$  at 20°C.

The best known temperature function is the Arrhenius function, leading to a temperature factor :

$$g(\theta) = \exp \left[ \frac{E}{R} \left( \frac{1}{293} - \frac{1}{273 + \theta} \right) \right] \quad (4)$$

with  $R = 0.00831 \text{ kJ/molK}$  = the universal gas constant.

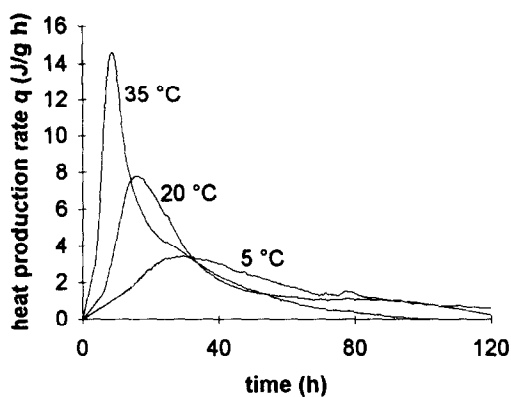


FIG. 3  
Heat production rate  $q(t)$

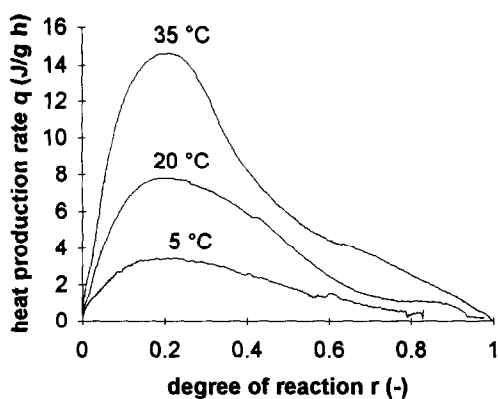


FIG. 4  
Heat production rate  $q(r)$

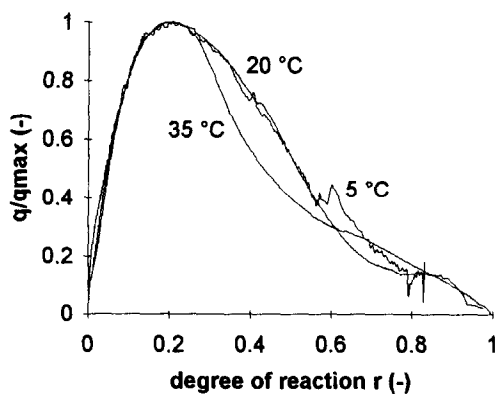


FIG. 5  
Standardized curves  $q/q_{\max}$

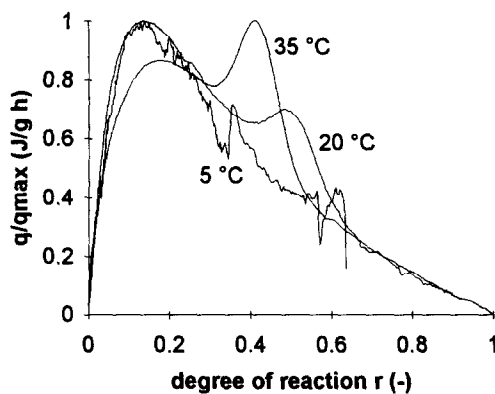


FIG. 6  
Standardized curves  $q/q_{\max}$

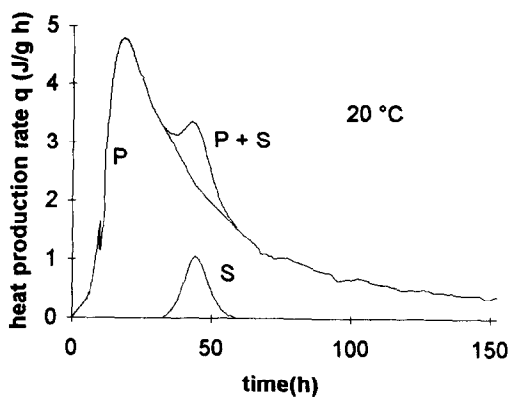


FIG. 7  
Superposition principle

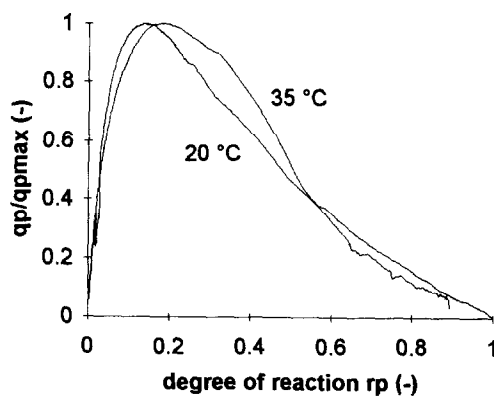


FIG. 8  
Standardized curves  $q_p/q_{p\max}$

For the tested portland cement the apparent activation energy  $E$  is found to be 33.5 kJ/mol. Combination of equations (3), (4) and (5) yields a hydration model for portland cement :

$$q(r, \theta) = q_{\max, 20} \cdot f(r) \cdot g(\theta) \quad (5)$$

The heat production rate  $q$  is calculated as a function of the actual temperature  $\theta$  and the degree of reaction  $r$ . The temperature influence on the heat production rate seems to be completely independent from the influence of the degree of reaction. Both influences are described separately by two different functions.

### 3.2. Blast furnace slag cement CEM III/B 32.5 and CEM III/C 32.5

When applying the same principles to the blast furnace slag cements (for example for CEM III/B 32.5), the situation of Figure 6 is obtained. Obviously, in contrast with portland cement, for the slag cement a single function for describing the effect of the state of the hardening process on the heat production does not exist. The reason can be found in the fact that the hydration of slag cement is composed of two reactions : a portland reaction (P-reaction) and a slag reaction (S-reaction). The slag is activated by the lime made available during the hydration of the portland cement fraction. From the literature (6, 7) it is known that both reactions have different temperature factors. The slag reaction is more sensitive to heat than portland cement clinker. This follows also from Figure 6 and explains why a unique, temperature independent function  $f(r)$  does not exist for slag cement.

A new approach for dealing with this problem is based on the two-fold character of the hydration reaction of slag cement : P-reaction and S-reaction. It is assumed that, for the heat production rate  $q$ , a superposition is possible of the P- and S-reactions. As indicated in Figure 7, the heat production of the slag cement can be divided in two separate contributions, corresponding with the P-reaction and S-reaction. Applying this superposition principle on the results for the different test temperatures, and standardizing the P- and S-reaction separately, Figures 8 and 9 are obtained.

The standardized curves for the P-reaction are very similar to those obtained for the portland cement. The curves for the S-reaction seem to be more symmetric, and indicate that the S-reaction ends more rapidly. The issue of the chemical reactivity of slag in cement paste during hydration has already been raised by Roy and Idorn (6). They observed that the transport of water through a blast furnace slag cement mortar practically comes to a stand-still after a certain hardening time. Moreover, the alkalis and lime, released by the residual portland cement, are retained in the hydration products of the slag fraction, and do not seem to contribute to the hydration of the slag (6).

The previous considerations for the slag cement CEM III/B 32.5 lead to a new general hydration model based on the superposition of the heat production of the P-reaction and S-reaction :

$$q = q_P + q_S \quad (6)$$

with  $q_P$  = heat production rate of the P-reaction  
 $q_S$  = heat production rate of the S-reaction

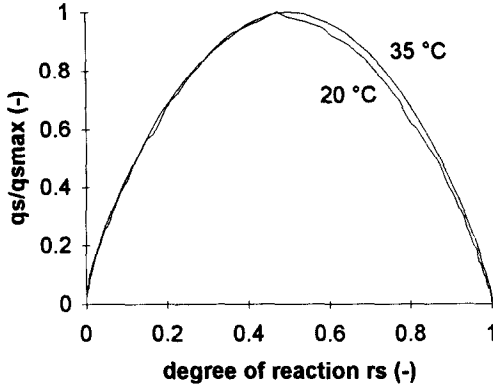


FIG. 9  
Standardized curves  $q_s/q_{smax}$

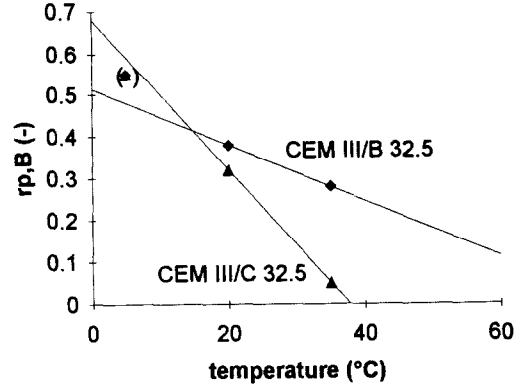


FIG. 10  
Threshold value  $r_{p,B}$

For the P-reaction the formulation is very similar with the formula's given for the portland cement CEM I 52.5 :

$$q_P = q_{P,max,20} \cdot f_P(r_P) \cdot g_P(\theta) \quad (7)$$

$$f_P(r_P) = c_P \cdot [\sin(r_P \pi)]^{a_P} \cdot \exp(-b_P \cdot r_P) \quad (8)$$

$$g_P(\theta) = \exp \left[ \frac{E_P}{R} \left( \frac{1}{293} - \frac{1}{273 + \theta} \right) \right] \quad (9)$$

with  $q_{P,max,20}$  = maximum heat production rate of the P-reaction, at 20°C  
 $r_P$  = degree of reaction of the P-reaction  
 $a_P, b_P, c_P$  = constants  
 $E_P$  = apparent activation energy of the P-reaction

The S-reaction can be described mathematically as follows :

$$q_S = q_{S,max,20} \cdot f_S(r_S) \cdot g_S(\theta) \quad (10)$$

$$f_S(r_S) = [\sin(r_S \pi)]^{a_S} \quad (11)$$

$$g_S(\theta) = \exp \left[ \frac{E_S}{R} \left( \frac{1}{293} - \frac{1}{273 + \theta} \right) \right] \quad (12)$$

with  $q_{S,max,20}$  = maximum heat production rate of the S-reaction, at 20°C  
 $r_S$  = degree of reaction of the S-reaction  
 $a_S$  = constant  
 $E_S$  = apparent activation energy of the S-reaction

The degrees of reactions  $r_P$  and  $r_S$  can be calculated by means of an expression similar to

equation (1) :

$$r_p(t) = \frac{Q_p(t)}{Q_{p,max}} = \frac{1}{Q_{p,max}} \int_0^t q_p(t) dt \quad (13)$$

$$r_s(t) = \frac{Q_s(t)}{Q_{s,max}} = \frac{1}{Q_{s,max}} \int_0^t q_s(t) dt \quad (14)$$

In these equations  $Q_{p,max}$  respectively  $Q_{s,max}$  is the total heat released at the end of the P-reaction respectively S-reaction.  $Q_{p,max}$  and  $Q_{s,max}$  can be estimated by integrating the heat production curves obtained from the P- and S-reactions.

As can be seen from Figure 7 the S-reaction doesn't start immediately after water addition. The slag hydration only starts in the presence of a certain quantity of alkalis and lime, released by the hydrating portland clinker. This is implemented mathematically by keeping the second term,  $q_s$ , in equation (6) equal to zero as long as the degree of reaction of the P-reaction hasn't reached a threshold value  $r_{p,B}$ . The parameter  $r_{p,B}$  is temperature dependent (Figure 10). For the moment a linear relationship is applied, by lack of further test results :

$$r_{p,B} = A\theta + B \geq 0 \quad (15)$$

with A, B = constants.

A more refined relationship can only be based on a chemical investigation about the nature of  $r_{p,B}$ .

### 3.3. Conclusion from the isothermal hydration tests

The equations (6) to (12) constitute a new general hydration model. For the blast furnace slag cement CEM III/B 32.5 and CEM III/C 32.5 the values for the different model constants are given in table 3. It is remarked here that the activation energy  $E_p$  or  $E_s$  found for different cements is quite different. This is hard to understand, and needs some further investigation. As the equations given for the P-reaction are identical to the hydration model developed for the Portland cement CEM I 52.5, it can be concluded that the hydration model (6) to (12) is valid both for Portland cement and for blast furnace slag cements. For portland cement it suffices to keep  $q_s$  always equal to zero, as the S-reaction has no significance in this case. Also for the portland cement CEM I 52.5 the values of the appropriate model constants are summarized in table 3. When the models are used in a numerical simulation procedure for hardening concrete, the degrees of reaction  $r_p$  and  $r_s$  should be initialized at a very small value, e.g. 0.001, instead of zero.

## 4. RESULTS OF THE ADIABATIC HYDRATION TESTS

Figure 11 gives the adiabatic temperature history obtained for the blast furnace slag cement CEM III/B 32.5 using the test equipment shown in Figure 2. Assuming a specific heat equal



TABLE 3  
Model constants

	CEM I 52.5	CEM III/B. 32.5	CEM III/C 32.5
$a_p$	0.667	0.667	0.5
$b_p$	3.0	3.5	2.5
$c_p$	2.5968	2.8461	2.1425
$q_{p,max,20}$ (J/gh)	7.79	4.80	1.42
$Q_{p,max}$ (J/g)	270.0	251.0	167.0
$E_p$ (kJ/mol)	33.5	45.0	55.0
$a_s$	-	0.667	0.667
$q_{s,max,20}$ (J/gh)	-	1.06	0.62
$Q_{s,max,20}$ (J/g)	-	11.3	32.5
$E_s$ (kJ/mol)	-	80.0	45.0

to 1000 J/kg°C, the adiabatic temperature curve can be simulated by means of the newly developed hydration model outlined in Section 3. As shown in Figure 11 simulation and experiment agree very well. The accuracy of the superposition model (6) becomes even more clear when looking at the heat production rate  $q$  during the adiabatic hydration test (Figure

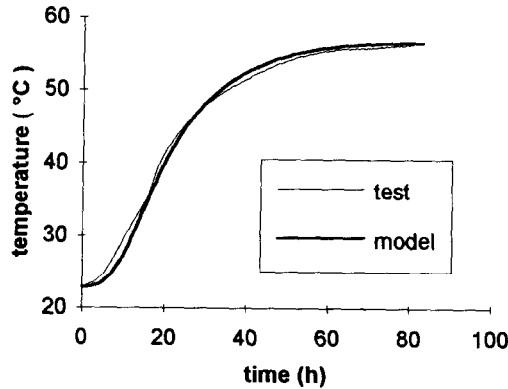


FIG. 11  
Adiabatic hydration curve

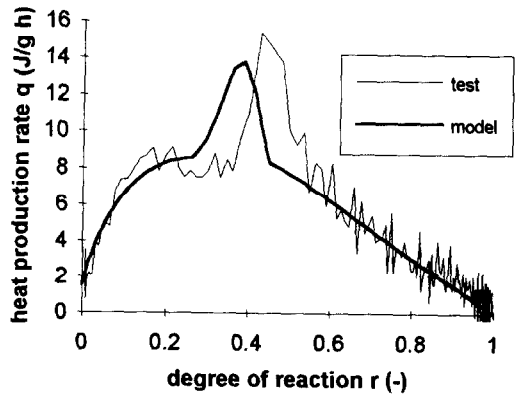


FIG. 12  
Heat production rate during adiabatic test

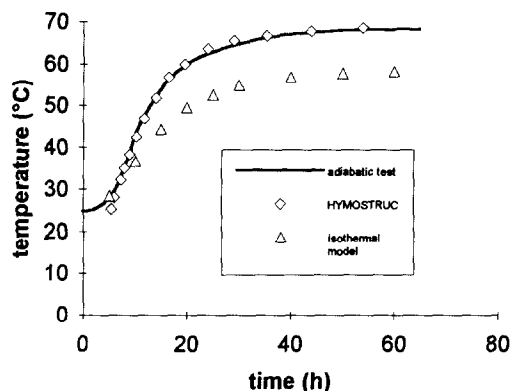


FIG. 13  
Adiabatic hydration curve

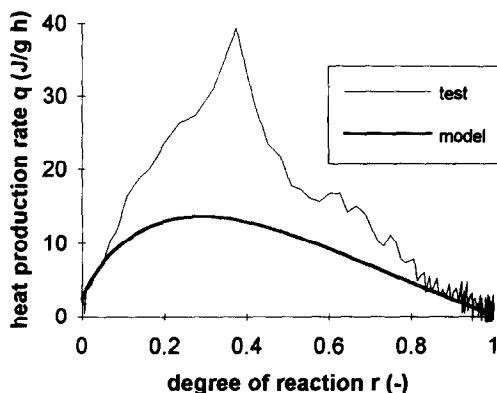


FIG. 14  
Heat production rate during adiabatic test

12). The peak corresponding to the slag part of the reaction seems to be simulated in a very accurate way.

For the Portland cement CEM I 52.5 the experimentally obtained adiabatic curve is given in Figure 13. A theoretical adiabatic hydration curve for this cement was provided by Van Breugel. By means of his simulation program HYMOSTRUC (8) a lower bound calculation was made, which agrees reasonably well with the experimental result. The differences occurring during the first hours are completely due to the fact that the dormant period is not implemented in HYMOSTRUC.

A comparison between the experimentally obtained adiabatic curve and a simulation based on the hydration model developed in Section 3 is less satisfactory (Figure 13). From Figure 14, which gives the heat production rate during the adiabatic test, it can be seen that during the adiabatic test a peak occurs, with heat production rates up to almost 40 J/gh. This peak isn't found when extrapolating the results of the isothermal hydration tests to the higher temperature range of the adiabatic test. As the peak occurs at a temperature of about 40 to 50°C, a temperature range where no isothermal tests have been carried out, it can be suspected that it is a temperature dependent process. It might be a chemical reaction, with a very high heat production, taking place at higher temperatures only, or at least with a much higher intensity. Probably this phenomenon is correlated with the effect of high early age temperatures on the ultimate strength of concrete. The difference in final strength gives evidence to the conjecture of a difference in microstructure, which is probably caused by different chemical processes.

The observed heat production peak might result from the transformation of ettringite ( $3\text{CaO} \cdot \text{Al}_2\text{O}_3 \cdot 3\text{CaSO}_4 \cdot 32\text{H}_2\text{O}$ ) into monosulphate ( $3\text{CaO} \cdot \text{Al}_2\text{O}_3 \cdot \text{CaSO}_4 \cdot 14\text{H}_2\text{O}$ ) in the presence of  $3\text{CaO} \cdot \text{Al}_2\text{O}_3 \cdot 6\text{H}_2\text{O}$ . Bensted (3) indicates that only a  $\text{C}_3\text{A}$ -amount of more than 12 % results in a visible third hydration peak during a 20°C isothermal hydration test. This is in agreement with the isothermally obtained heat production curve for CEM I 52.5 ( $\text{C}_3\text{A} = 7.5\%$ ), which shows no third peak. Indication for a thermally accelerated transformation of ettringite into monosulphate can be found from Negro et al. (9). Temperatures in the range of 50°C stimulate the formation of colloidal ettringite and subsequently accelerate the formation of  $3\text{CaO} \cdot \text{Al}_2\text{O}_3 \cdot 6\text{H}_2\text{O}$  and monosulphate. According to Van Breugel (8) the volume changes associated with the conversion of ettringite into monosulphate might indeed somewhat affect the strength development.

Whether the mentioned chemical transformations really cause the observed phenomenon has still to be verified. However, it can be concluded that during adiabatic conditions, with temperatures above 40°C, the hydration process differs from the process at isothermal conditions with lower temperatures. Nevertheless, when for the portland cement CEM I 52.5 the values  $Q_{\max} = 350 \text{ J/g}$  and  $q_{p,\max,20} = 11.5 \text{ J/gh}$  are used instead of the values given in table 3, the adiabatic temperature curve can be simulated with good agreement by the general hydration model of section 3, as was verified in reference (1).

## 5. CONCLUSIONS

- In order to carry out adiabatic hydration tests on concrete a new test set up was developed. This test set up enables an accurate measurement of the adiabatic temperature curve by controlling the temperature of a water-ring surrounding the concrete using a differential thermostat.
- Based on isothermal and adiabatic hydration tests a new general hydration model was developed, valid both for portland cement and blast furnace slag cement. This hydration model enables the calculation of the heat production rate as a function of the actual temperature and the degree of hydration.

A comparison between isothermal and adiabatic hydration tests on portland cement CEM I 52.5 shows that at higher temperatures other chemical reactions take place, resulting in a different heat production curve. This might also correlate with the effect of high initial temperatures on the ultimate strength of concrete. A possible explanation is given in Section 4, though it still needs to be verified.

## 6. ACKNOWLEDGEMENT

This project is financed by the Flemish Ministry of Public Works, and by the Belgian National Fund for Scientific Research (N.F.W.O.). This financial support is greatly acknowledged, as well as the contribution of the Belgian Research Centre of the Cement Industry to this research project. The authors also wish to thank Dr. K. Van Breugel, for providing the theoretical adiabatic hydration curve for the portland cement CEM I 52.5, by means of his simulation program HYMOSTRUC.

## 7. REFERENCES

1. R. Dechaene, J. De Rouck, G. De Schutter, L. Taerwe, F. Van der Weeën, L. Van Damme, Thermal cracking in hardening concrete armour units, PIANC Bulletin, 82, 1994, pp. 61-69.
2. G. De Schutter, L. Taerwe, F. Van der Weeën, Experiment based prediction of thermal characteristics of hardening concrete, Proceedings of the Third International Workshop on Behaviour of Concrete Elements under Thermal and Hydral Gradients, Wissenschaftliche Zeitschrift HAB Weimar, 3./4./5. Heft, pp. 117-126.
3. J. Bensted, Some applications of conduction calorimetry to cement hydration, Advances in Cement Research, Vol. 1, No. 1, October 1987, pp. 35-44.
4. Y. Suzuki, N. Yokota, S. Harada, T. Sado, Applicability of adiabatic temperature rise for estimating time-dependent temperature changes in concrete structures, Durability of Construction Materials, RILEM, 1987, pp. 1190-1197.
5. H.-W. Reinhardt, J. Blauwendraad, J. Jongendijk, Temperature development in concrete structures taking account of state dependent properties, International Conference on

concrete at early ages, RILEM, Paris, 1982, pp. 211-218.

6. D.M. Roy, G.M. Idorn, Hydration, structure and properties of blast furnace slag cements, mortars and concrete, *ACI Journal*, Nov.-Dec. 1982, pp. 444-457.
7. X. Wu, D.M. Roy, C.A. Langton, Early stage hydration of slag-cement, *Cement and Concrete Research*, Vol. 13, 1983, pp. 277-286.
8. K. Van Breugel, Simulation of hydration and formation of structure in hardening cement-based materials, PhD.-thesis, Delft, 1991, and privately communicated unpublished data.
9. A. Negro, A. Bachiorrini, Expansion associated with ettringite formation at different temperatures, *Cement and Concrete Research*, Vol. 12, 1982, pp. 677-684.